

ChemComm

Accepted Manuscript



This is an *Accepted Manuscript*, which has been through the Royal Society of Chemistry peer review process and has been accepted for publication.

Accepted Manuscripts are published online shortly after acceptance, before technical editing, formatting and proof reading. Using this free service, authors can make their results available to the community, in citable form, before we publish the edited article. We will replace this *Accepted Manuscript* with the edited and formatted *Advance Article* as soon as it is available.

You can find more information about *Accepted Manuscripts* in the [Information for Authors](#).

Please note that technical editing may introduce minor changes to the text and/or graphics, which may alter content. The journal's standard [Terms & Conditions](#) and the [Ethical guidelines](#) still apply. In no event shall the Royal Society of Chemistry be held responsible for any errors or omissions in this *Accepted Manuscript* or any consequences arising from the use of any information it contains.

COMMUNICATION

A Ratiometric Biosensor for Metallothionein Based on Dual Heterogeneous Electrochemiluminescent Responses from TiO₂ Mesocrystals formed interface

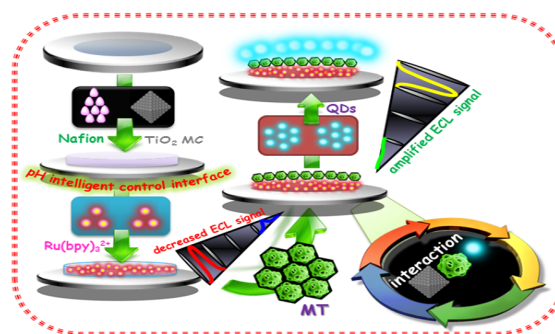
Hong Dai,^a Guifang Xu,^a Shupeizhang,^a Zhensheng Hong,^a Yanyu Lin^{a,b}

Herein, an ultrasensitive dual-signal electrochemiluminescent intelligent biosensor constructed by superstructure TiO₂ mesocrystals was proposed for metallothionein detection.

Metallothionein (MT) was firstly discovered from purification of a Cd-binding protein from horse kidney by Margoshens and Vallee in 1957.¹ It is a kind of intracellular proteins presenting cysteine-rich, low molecular weight and heavy metal-binding properties.¹⁻⁴ Some studies have found increased expression of MT in some cancers of the breast, colon, kidney, liver and so on.^{4,5} Moreover, MT levels was associated with certain brain diseases such as brain infarction, Parkinson's disease, and Alzheimer's disease.⁶ Therefore, MT has multiple roles in monitoring various diseases. Hitherto, various methods and strategies have been used to determine MT.^{2,7} However, these methods remain time-consuming, high cost, and complicate operate. More importantly, these methods are single signal detection, which always possess false-positive or false-negative results in complex matrix. Accordingly, it is significant to delve an accurate and inexpensive quantitative determination of MT.

Electrochemiluminescence (ECL) is a highly sensitive technique with low background signals and allows temporal and spatial controll,⁸ which has attracted considerable attention in various fields. However, the traditional ECL methods were designed on the basis of a change of single detection signal, which possessed some inevitable challenges by intensity fluctuations due to instrumental or environmental factors, especially at very low concentrations and in complex biological systems.⁹ Inspired by fluorescent ratiometric methods, these problems could be overcome by dual-response ECL detection.¹⁰ It is feasible to develop dual-signal ECL through potential scanning because of the controllability of emission from ECL emitter in the given potential range. Herein, the potential-resolved ECL strategy based on Ru(bpy)₃²⁺ and CdTe QDs is reasonable, but the challenge in immobilizing two luminophores on a electrode interface is still existed.

Mesocrystal, an intermediate between tradition polycrystal and ideal single crystal,¹¹ can be regarded as a favorable supplement to polycrystal and single crystal, resulting from it possesses the advantages of polycrystal and single crystal. Moreover, mesocrystals are porous structure, which are similar to zeolite.^{12,13} Therefore, mesocrystals not only maintain the properties of nanoparticles, but also exhibit new effects or improved properties, due to the large specific surface area and high crystallinity.¹³⁻¹⁶ In recent years, the



Scheme 1 A schematic illustration of the dual-response ECL sensor.

attention of chemists and physicists was focused on mesocrystals, especially TiO₂ mesocrystals (TiO₂ MC). To extend the application fields of TiO₂ MC, we used TiO₂ MC to establish the dual-response ECL sensor. The fabrication procedure of the device was presented in Scheme 1. On the basis of porous TiO₂ MC, the sensing interface could immobilized more Ru(bpy)₃²⁺ by the ion exchanging technology, and the outer Helmholtz plane (OHP) of the sensing interface was extended, resulting in more redox reactions of Ru(bpy)₃²⁺ occurred at the modified electrode.¹⁷ On the other hand, TiO₂ MC could make the pH in the nanocomposite film higher, leading to Ru(bpy)₃²⁺ possessing strong ECL intensity in moderate condition. In addition, TiO₂ MC can be employed to link MT, because of the strong interaction between -SH and TiO₂ MC. This stable interaction was attributed to the formation of a bond between thiol group and surface Ti⁴⁺ cation of TiO₂ MC. Furthermore, the hydrogen bond between the MT and TiO₂ MC could cooperate with S-Ti to make MT assemble tightly on the surface of TiO₂ MC.¹⁸ The extended part of MT was associated with CdTe QDs via Cd-S bond, resulting in the cathode ECL from CdTe QDs. Consequently, the dual-response ECL sensing strategy developed by the TiO₂ MC-dependent MT-regulated ECL emissions of Ru(bpy)₃²⁺ and CdTe QDs as two different ECL emitters was successfully established in this work. Moreover, the ECL images at the two excitation potentials were recorded, which could lay the foundation for simultaneously visualized detection. Additionally, the MT biosensor-based logic gate strategy was designed. Therefore, this designed strategy based on TiO₂ MC provided new opportunities for development of biosensor systems for logic gate computation and

sensing applications in the future and exhibit good analytical performance in clinical diagnosis.

TiO₂ MC was successfully synthesized and various characteristic techniques were provided to insight into the morphologies and structures of TiO₂ MC in Fig.S-1. To further investigate the nanomaterial, the electrochemical behaviors of the immobilized Ru(bpy)₃²⁺ ECL sensor were collected in Fig. 2A, which showed that electrochemical response of the Nafion-TiO₂ MC/Ru(bpy)₃²⁺/GCE was larger than that case at Nafion/Ru(bpy)₃²⁺/GCE. According to the anodic peak area, the surface coverage amount of Ru(bpy)₃²⁺ immobilized on the Nafion-TiO₂ MC/GCE was 1.6 times more than that on Nafion/GCE. Additionally, the ECL signals of the modified electrodes were also obtained in Fig.2A, which were consistent with the results of electrochemical responses. These revealed that TiO₂ MC offered high surface area and excellent porosity, leading to more Ru(bpy)₃²⁺ immobilized on the Nafion-TiO₂ MC/GCE. Moreover, the porous TiO₂ MC with high surface area extended the OHP,¹⁷ resulting in more redox reactions of Ru(bpy)₃²⁺ occurred at the modified electrode. To further confirm the opinion, the time of Ru(bpy)₃²⁺ immobilization as one of significant factors relevant to the ECL response was shown in Fig.S-2A. The phenomenon was similar to that above, indicating the porous TiO₂ MC could provide high surface area and excellent porosity to immobilize more Ru(bpy)₃²⁺ on the Nafion-TiO₂ MC/GCE and effectively extend OHP of the sensing interface to amplify the signal of the ECL sensor. In addition, the TiO₂ MC offered another merit which could make the pH in the composite film higher, resulting in Ru(bpy)₃²⁺ possessing strong ECL intensity in moderate condition, which was confirmed by the demonstration as below.

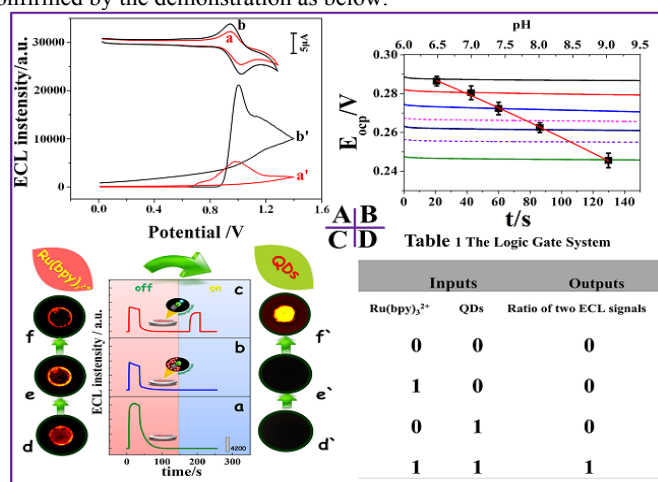


Figure 2 (A) CV curves of Nafion/Ru(bpy)₃²⁺/GCE(a), Nafion-TiO₂ MC/Ru(bpy)₃²⁺/GCE(b), ECL of different electrodes, Nafion/Ru(bpy)₃²⁺/GCE(a'), Nafion-TiO₂ MC/Ru(bpy)₃²⁺/GCE(b'); (B) Potential response in time of a potentiostatically deposited IrO_x on GCE in various buffer solutions. E_{OCP} vs time measured at an IrO_x/Nafion/GCE (magenta dashed line), IrO_x/Nafion-TiO₂ MC/GCE (violet dashed line). (C) ECL of different electrodes, Nafion-TiO₂ MC/Ru(bpy)₃²⁺/GCE(a), Nafion-TiO₂ MC-MT/Ru(bpy)₃²⁺/GCE (b), Nafion-TiO₂ MC-MT-CdTe/Ru(bpy)₃²⁺/GCE(c) in 0.1 M PBS containing 5mM K₂S₂O₈, the ECL images (d), (e), (f), (d'), (e'), (f'); (D) Table 1 the logic gate system.

The pH was measured by pH-sensitive iridium oxide (IrO_x) electrode,¹⁸ and its open circuit potential E_{OCP} was investigated in Fig.2B. The E_{OCP} responses indicated a linear response was obtained in the pH range from 6.5 to 9.0 with a slope of -0.0167 V/pH. Therefore, the calibration plot of E_{OCP} vs pH was established successfully. When Nafion was casted on the surface of IrO_x electrode, the effect of Nafion overcoat on the pH was determined (magenta dashed line), showing the open circuit potential shifted

toward the negative value. Such shift in E_{OCP} indicated the increase in the pH of the film, which resulted from the Nafion overcoat precluded the escape of dianion based on Donnan exclusion principle, leading to increasing the concentration ratio [HPO₄²⁻]/[H₂PO₄⁻] to enhance the value of pH.¹⁹ Besides, when Nafion-TiO₂ MC composite film was coated on the IrO_x electrode, the open circuit potential shifted to the more negative value, as shown in Fig.2B (violet dashed line). It suggested the value of pH underlying film was near to 8.5, which was higher than before. The increase in pH beneath the Nafion-TiO₂ MC film had two reasons. On one hand, TiO₂ MC possessed porosity and high surface area, which could enhance the surface area of the composite film. Then it could preclude more dianion to escape and facilitate the charge transport. On the other hand, there were many -OH functional groups on the surface of TiO₂ MC. Moreover, Nafion possessed lots of F⁻, leading to the increased generation of OH⁻ because of fluoride displacement of the surface OH⁻ groups on the TiO₂ MC, which in well accordance with previous study.²⁰ Therefore, the pH in the composite film was higher, making Ru(bpy)₃²⁺ possess stronger ECL intensity at the moderate condition. Accordingly, it has promising applications for establishing biosensors under physiological conditions.

To investigate the behavior of the ECL sensors, the potential-resolved ECL intensity was recorded in Fig.2C. The multi-potential steps oscillating from 1.2 to -1.4 V was applied. Comparing with the ECL performance of different modified electrodes, the ECL intensity was the strongest at Nafion-TiO₂ MC/Ru(bpy)₃²⁺/GCE (Fig.2C(a)), due to the porous TiO₂ MC that was beneficial to immobilize more Ru(bpy)₃²⁺ on the electrode, and extend the OHP to accelerate the redox reaction of Ru(bpy)₃²⁺. The performance displayed that Ru(bpy)₃²⁺ was no emission at the negative potential (-1.4V). However, the ECL intensity at Nafion-TiO₂ MC/Ru(bpy)₃²⁺/GCE decreased dramatically (Fig. 2C(b)), demonstrating that MT was successfully immobilized on the Nafion-TiO₂/Ru(bpy)₃²⁺/GCE through Ti-S bond. The large molecular MT not only blocked the electron transfer, but also obstructed the co-reactant to diffuse onto the electrode. As expected, the ECL intensity of the Ru(bpy)₃²⁺ further reduced and the ECL emission at negative potential (-1.4 V) appeared in Fig.2C(c) after CdTe QDs which could produce ECL response at negative with peroxydisulfate as the co-reactant were assembled on the modified electrode via the covalent interaction between -SH of MT and CdTe QDs.²⁻⁴ Moreover, the corresponding ECL images of various modified electrodes were recorded in Fig.2C, and the phenomenon was consistent with the aforementioned result, providing visible impression for ECL signals of different modified electrodes. As Fig.S-2B shown, electrochemical impedance was also carried out to further characterise various modified electrodes, which indicated that the dual-signal ECL sensor was established successfully. Therefore, these phenomena strongly proved TiO₂ MC and Nafion composite film could be a promising ECL platform for sensitive sensing and visible detection. In addition, these results certified dual-response ECL sensor on the single electrode was successfully established. It provides new opportunities for simultaneously detecting multi-analytes on the single electrode and possesses well potential application in various fields.

Upon the optimized conditions, as shown in Fig.S-2 and Fig.S-3, a dual-response ECL immunosensor for MT was developed with sensitive detection and wide dynamic response range. The analytical reliability and real application of biosensor was demonstrated in Fig. 3A. With the increase of the concentration of MT, the ECL from Ru(bpy)₃²⁺ decreased and the ECL from CdTe QDs increased correspondingly. Moreover, the lg(ECL_{Ru(bpy)3²⁺}/ECL_{QDs}) was found to be logarithmically related to the concentration of MT in the range from 5 to 10000 ng/mL in Fig. 3B. The limit of detection(LOD) with 1.67 ng/mL in this communication was lower than previous studies.^{2,21} Besides, the proposed biosensor was expended readily for

detecting the amount of MT in practical analytical applications. The results were shown in Table S-2. Fig.3C displayed the dual-response ECL of modified electrode under ten times and the relative standard deviation for ten parallel measurements with proposed sensor was 5.30%, indicating an excellent precision. The life time of this dual-signal ECL biosensor is also a key factor in its application and development. When the sensor was dried and stored at 4 °C, it retained 90% of its initial response after a storage period of 30 days, indicating the proposed sensor had stable storage stability. Then the selectivity of the present dual-signal ECL biosensor was also ascertained using some other proteins as potential interfering agents. As the Fig.3D revealed, the present biosensor showed an excellent selectivity for MT over other proteins. Moreover, the method was a new concept of the phenomenon of MT logic gate. It was the first MT driven dual-signal ECL logic gate. The logic gate was represented by the situation where the output of the gate occurred when the both QDs and Ru(bpy)₃²⁺ appeared. As showed in Fig.2D, the experiments were exhibited by studying the logic gate with four possible input combination involving (0,0) (1,0), (0,1) and (1,1). The present of QDs or Ru(bpy)₃²⁺ was defined as 1 and the absence as 0. The ratio of the two electrochemiluminescent signals acted as the output (1 or 0). When both QDs and Ru(bpy)₃²⁺ presented in a sample (1,1), the logic gate turned on and the ratio of the two ECL signals was produced (output 1). When one (0, 1 or 1, 0) or neither (0, 0) of the ECL reagents was present, no ratio of the two signals showed (output 0). Therefore, the proposed dual-response ECL device was served as an excellent biosensor and had potential applications in other biological systems. Furthermore, the concept of the performance of MT logic gate could open the new chances for development and design of logic gate sensing applications in the future.

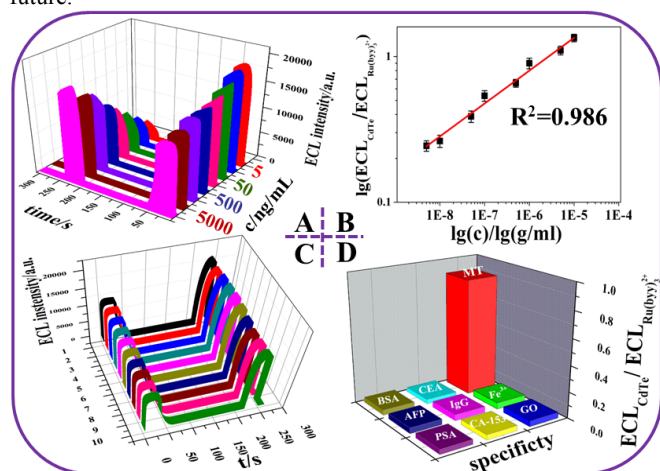


Figure 3 (A) ECL signal-time curves at the dual potential ECL sensing interface with MT from different concentrations: 5ng/mL, 10ng/mL, 50ng/mL, 100ng/mL, 500ng/mL, 1000ng/mL, 5000ng/mL, 10000 ng/mL, (B) Relationship between the log (ECL_{CdTe}/ECL_{Ru(bpy)₃²⁺}) and log (the concentration of MT), (C) Stability of the dual-signal ECL biosensor, (D) Selectivity of the dual-signal ECL biosensor, high-concentration interferents (500ng/mL) and low-concentration MT (100ng/mL).

In summary, a dual-response ECL sensing platform was designed for metalloethionein determination based on TiO₂ MC. The results exhibited the change of ECL responses was associated with the concentration of MT, then the ratio of the two ECL signals was used to judge the accuracy of detecting MT to avoid the false positive or negative results and improve the accuracy. The dual-signal ECL sensor towards MT with excellent stability and selectivity was established. Additionally, the LOD of this sensing strategy could be down to ng/mL, and the dynamic response range of this biosensor could cross four orders of magnitude. Moreover, it also could be

successfully applied in detecting MT in the real samples. Furthermore, the ECL images at the two excitation potentials were recorded. Therefore, this method was a promising format for the future development of multiplex ECL biosensors and simultaneously visualized detection in a complicated environment.

This project was financially supported by the NSFC (21205016).

Notes and references

^a College of Chemistry and Chemical Engineering, Fujian Normal University, Fuzhou 350108, P. R. China

^b Ministry of Education Key Laboratory of Analysis and Detection for Food Safety, and Department of Chemistry, Fuzhou University, Fuzhou 350002, P. R. China

E-mail: dhong@fjnu.edu.cn (H. Dai); winter0514@163.com (Z. Hong) Fax: (+86)-591-22866135

† Electronic supplementary information (ESI) available: experimental details. See DOI: 10.1039/b000000x/

References

- J. Petrlova, S. Krizkova, O. Zitka, J. Hubalek, Prusa, R., V. Adam, and J. Wang, *Sensors and Actuators B*, 2007, **127**, 112-119.
- N. Kim, S. H. Shon, C. T. Kim, Y. J. Cho, and C. J. Kim, *Current Applied Physics*, 2011, **11**, 1210-1214.
- S. Skalicikova, O. Zitka; L. Nejdil, S. K. J. Sochor, L. Janu, M. Ryvolova, D. Hynek, J. Zidkova, V. Zidek, V. Adam, and R. Kizek, *Chromatographia*, 2013, **76**, 345-353.
- M. D. Wicherek, A. Lazar, R. Tomaszewska, W. Kazmierczak, and L. Wicherek, *Cell Tissue Res*, 2013, **352**, 341-349.
- Z. Tian, X. Wang, W. Wu, B. Li, and Y. Wang, *Chin. J. Cancer*, 2008, **27**, 160-164.
- Y. Uchida, K.Takio, K. Titani, Y. Ihara, and M. Tomonaga, *Neuron*, 1991, **7**, 337-347.
- (a) T. Minami, S. Ichida, and K. Kubo, *J. Chromatogr. B*, 2002, **781**, 303-311. (b) J. Garvey, *Environ. Health. Perspect.*, 1984, **54**, 117-127.
- (a) Z. X. Wang, C. L. Zheng, Q. L. Li, *Analyst*, 2014, **139**, 1751-1755. (b) H. P. Huang, J. J. Li, and J. J. Zhu, *Anal. Methods*, 2011, **3**, 33-42.
- M. Takeuchi, Y. Nagaoka, T. Yamada, H. Takakura, and T. Ozawa, *Anal. Chem.*, 2010, **82**, 9306-9313.
- (a) H. R. Zhang, J. J. Xu, H. Y. Chen, *Anal. Chem.* 2013, **85**, 5321. (b) H. R. Zhang, M. S. Wu, J. J. Xu, H. Y. Chen, *Anal. Chem.*, 2014, **86**, 3834-3840. (c) N. Hao, X. L. Li, H. R. Zhang, J. J. Xu, H. Y. Chen, *Chem Commun*, 2014, **50**, 14828-14830.
- H. M. Lv, X. F. Yang, Y. G. Zhong, Y. Guo, Z. Li, and H. Li, *Anal. Chem.*, 2014, **86**, 1800-1807.
- M. Grzelczak, J. Vermant, E. M. Furst, and L. M. Liz-Marzn, *ACS Nano*, 2010, **4**, 3591-3605.
- R. Q. Song, H. Colfen, *Adv. Mater.*, 2010, **22**, 1301-1330.
- Z. S. Hong, Y. X. Xu, Y. B. Liu, and M. D. Wei, *Chem. Eur. J.*, 2012, **18**, 10753-10760.
- P. Tartaj, J. M. Amarilla, *Adv. Mater.*, 2011, **23**, 4904-4907.
- (a) D. K. Zhong, D. R. Gamelin, *J. Am. Chem. Soc.*, 2010, **132**, 4202-4207. (b) K. Sivula, F. Le Formal, and M. Gratzel, *Chem. Sus. Chem.*, 2011, **4**, 432-449. (c) M. Armand, J. M. Tarascon, *Nature*, 2008, **451**, 652-657.
- (a) S. P. Du, Z. Y. Guo, B. B. Chen, Y. H. Sha, X. H. Jiang, X. Li, N. Gan, and S. Wang, *Biosensors and Bioelectronics*, 2014, **53**, 135-141. (b) A. J. Bard, L. R. Faulkner, *Electrochemical Methods: Fundamentals and Applications*, 2nd ed. Wiley New York, 2000.
- (a) W. Langel, L. Menken, *Surf. Sci.* 2003, **1**, 538. (b) J. M. R. Muir, H. Idriss, *Surf. Sci.* 2013, **617**, 60.
- (a) S. Karra, W. Gorski, *Anal. Chem.*, 2013, **85**, 10573-10580. (b) E. P. Alfonso, L. Abad, N. C. Pastor, J. G. Ruiz, and E. Baldrich, *Biosensors and Bioelectronics*, 2013, **39**, 163-169.
- Y. M. Xu, K. L. Lv, Z. G. Xiong, W. H. Leng, W. P. Du, D. Liu, and X. J. Xue, *J. Phys. Chem. C*, 2007, **111**, 19024-19032.
- (a) N. Kima, S. H. Sona, C. T. Kima, Y. J. Choa, C. J. Kima, and W. Y. Kimb, *Sensors and Actuators B*, 2011, **157**, 627-634. (b) W. Tang, T. Kido, W. A. Gross, K. Nogawa, E. Sabbioni, and Z. A. Shaikh, *Anal. J. Toxicol.*, 1999, **23**, 153-158. (c) S. Miyairi, S. Shibata, and A. Naganuma, *Anal. Biochem.*, 1998, **258**, 168-175.